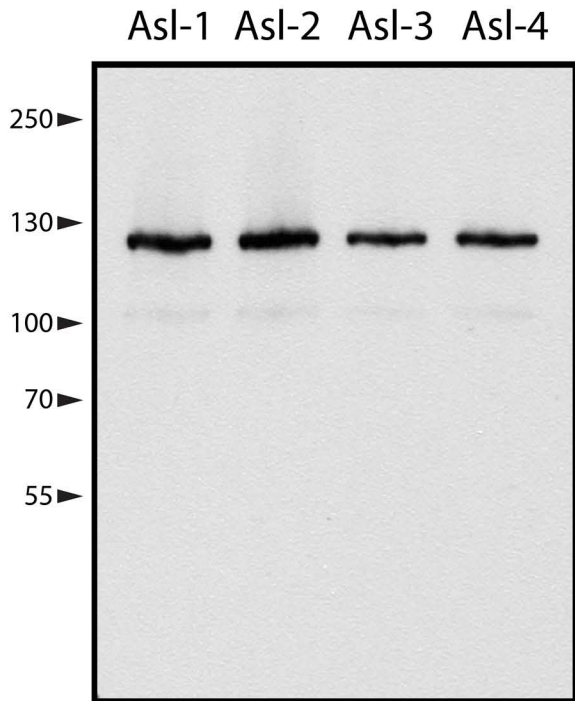
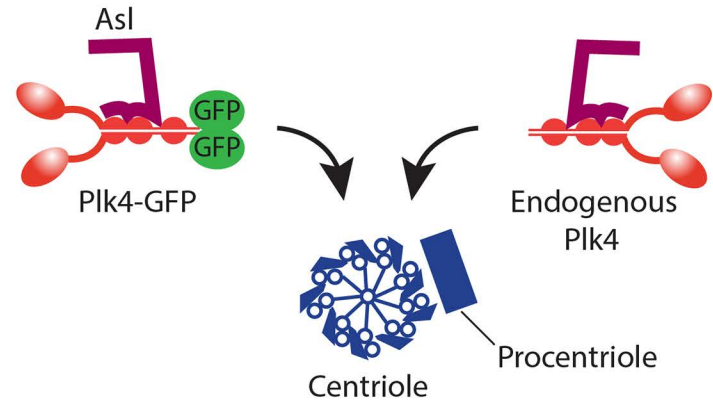


Figure S1

A



B. Wild-type Plk4-GFP expression



C. Kinase-dead (KD) Plk4-GFP expression

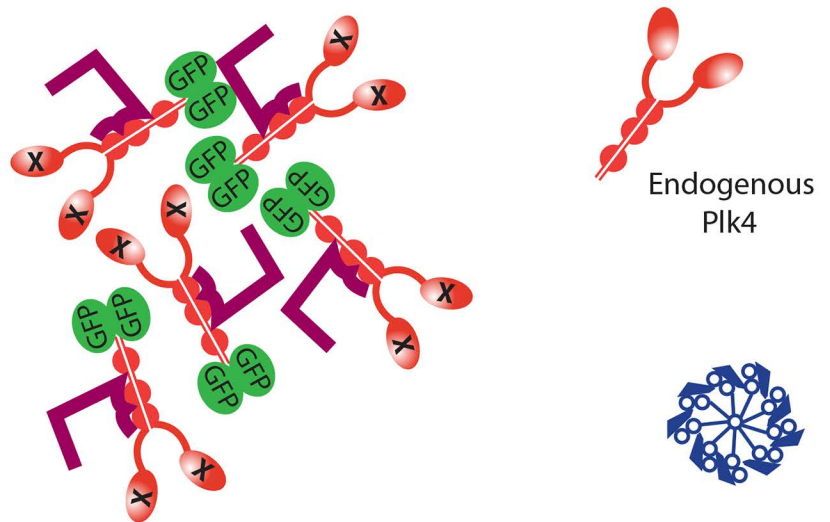


Figure S1. Kinase-dead Plk4 Could Exert its Dominant/Negative Effect on Centriole Duplication in *Drosophila* by Sequestering Asterless

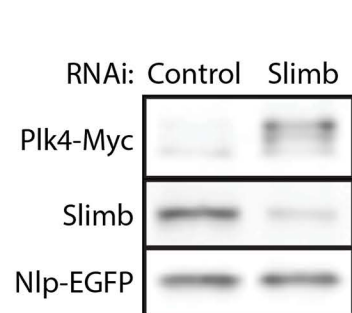
(A) Anti-Asterless (Asl) antibodies used in this study are specific. Four different guinea pig polyclonal anti-Asl antibodies were raised against purified recombinant full-length GST-Asl and affinity-purified against MBP-Asl. The specificity of these antibodies (Asl-1-4) on immunoblots against S2 cell lysates is shown. All antibodies react with the identical ~125 kDa polypeptide and immunostain centrioles in S2 cells (see Figure 1D).

(B) High expression of wild-type (WT)-Plk4-EGFP in S2 cells drives centriole amplification. Plk4 (both endogenous and transgenic) (red) binds endogenous Asterless (Asl) (purple) through its Polo Boxes (PB) 1 and 2 (aka 'the Cryptic Polo Box'). Asl then targets Plk4 to the centriole (blue) surface where it initiates centriole duplication (procentriole assembly).

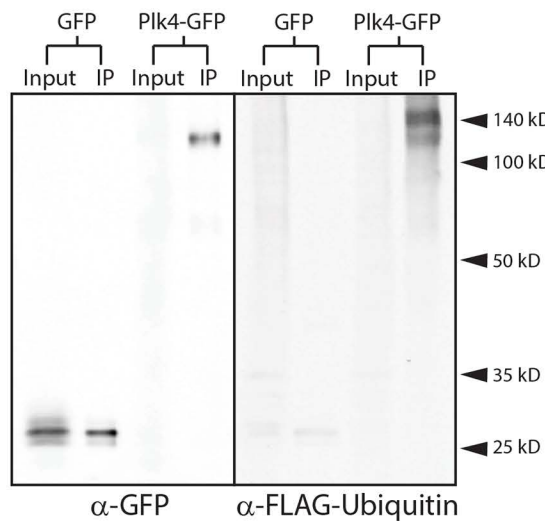
(C) High expression of kinase-dead (KD)-Plk4-EGFP (red, marked with 'X') in S2 cells inhibits centriole duplication. KD-Plk4 binds endogenous Asl and forms cytoplasmic aggregates. By sequestering Asl and preventing it from localizing to centrioles, centriole duplication is blocked. Likely, this is due to the inability of endogenous Plk4 to target centrioles. However, Asl is a multi-functional scaffolding protein and may play additional unidentified roles in the duplication process. This dominant/negative effect on centriole duplication is specifically due to sequestering Asl because it is rescued by expression of KD-Plk4 lacking the Asl-binding domain (delta-PB1-PB2) (not shown in this illustration).

Figure S2

A

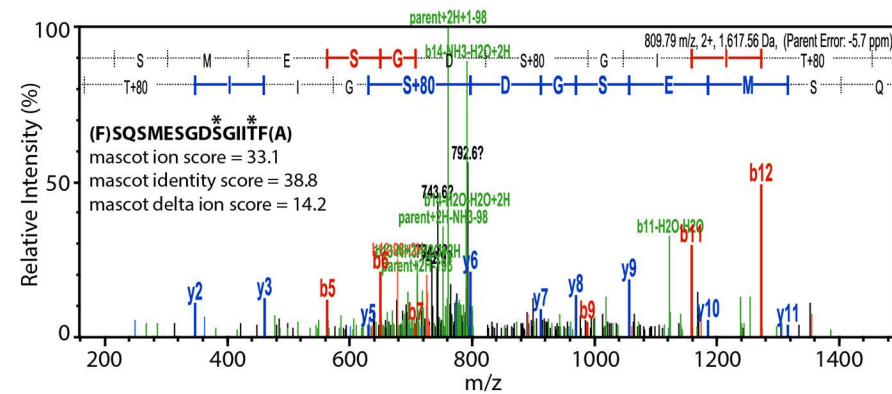


C

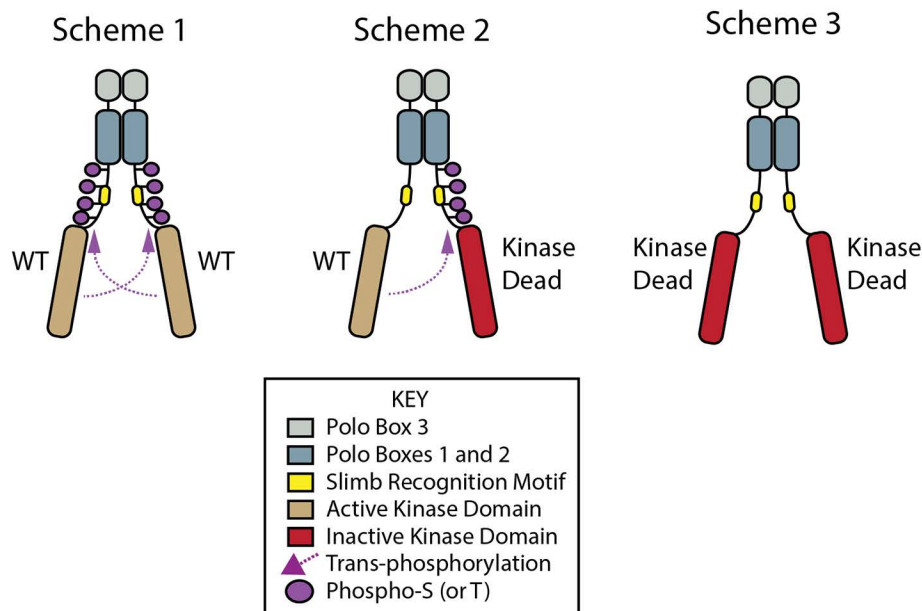


D

In Vitro Phosphorylated



B



E

In Vivo Phosphorylated

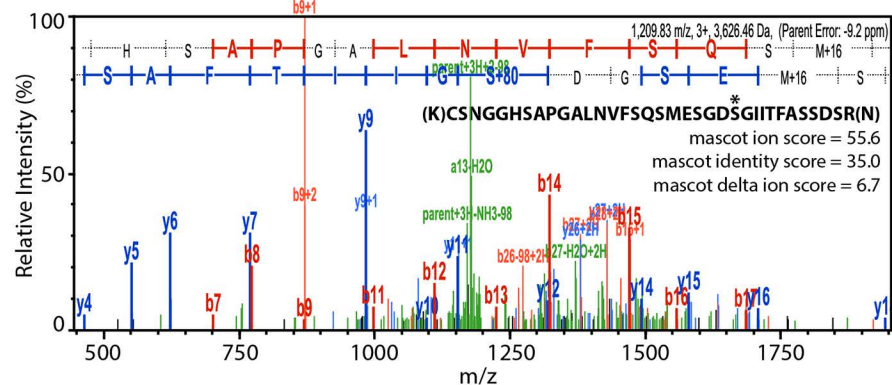


Figure S2. Plk4 Trans-Autophosphorylation is Probably Primarily Responsible for the Phosphorylation of the Downstream Regulatory Element (DRE) In Vitro and In Vivo

(A) Immunoblots of lysates from control or Slimb-depleted S2 cells transiently co-expressing Plk4-Myc and Nlp-EGFP (loading control). Slimb-depletion was used to stabilize the expressed Plk4-Myc, making the protein readily apparent and demonstrating that Plk4-Myc is expressed in transfected cells.

(B) Models depicting Plk4 dimerization scenarios. (1) Homodimerization of WT-Plk4 leads to trans-autophosphorylation, promoting Slimb-mediated ubiquitination of Plk4 and subsequent degradation of both molecules. (2) If WT-Plk4 heterodimerizes with KD-Plk4, then only KD-Plk4 is trans-phosphorylated leading to KD-Plk4 ubiquitination and degradation. (3) KD-Plk4 homodimerization is predicted to block phosphorylation, ubiquitination and degradation.

(C) 3xFLAG-tagged ubiquitin (Ubi) specifically labels Plk4-GFP but not GFP. Anti-GFP immunoprecipitates of lysates prepared from S2 cells transiently expressing 3xFLAG-ubiquitin and either EGFP or Plk4-EGFP were probed with anti-GFP and FLAG antibodies.

(D, E) Samples of Plk4 were prepared for MS analysis from either in vitro autophosphorylated Plk4 (D) or transgenic Plk4-EGFP immunoprecipitated from S2 cell lysates (E). To prepare the in vitro sample (D), bacterially expressed and purified Plk4-DRE-His₆ containing only the kinase domain and DRE (amino acids 1-317) was incubated with MgATP and then resolved by SDS-PAGE. The band corresponding to Plk4 was cut from the gel, processed, and then analyzed by tandem mass spectrometry (MS). An example of a mass spectrum obtained from the analysis of in vitro autophosphorylated Plk4 is shown (D). The sequence of the peptide is shown in bold; the phosphorylated residues (S293 and T297) are indicated with asterisks. (We note that this spectrum only weakly demonstrates T297 phosphorylation; however, other spectra verify the

phosphorylation of this residue.) To prepare the in vivo sample (E), S2 cells were transfected with Plk4-EGFP-encoding plasmid, and then the transgenic Plk4 was immunoprecipitated from S2 cell lysates, resolved by SDS-PAGE and similarly processed for tandem MS. An example of a mass spectrum obtained from the analysis of in vivo phosphorylated Plk4 is shown (E). The sequence of the peptide is shown in bold; the phosphorylated residue (S293) is indicated with an asterisk.

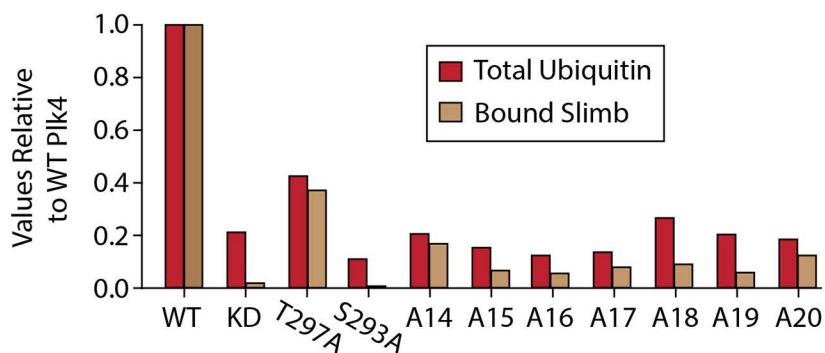
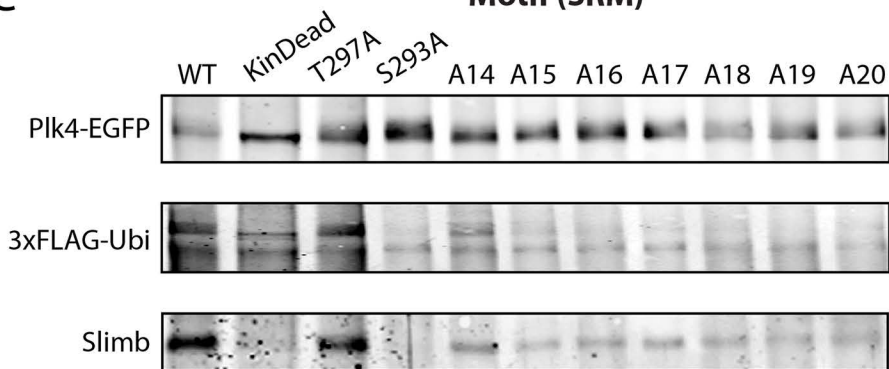
Figure S3

A

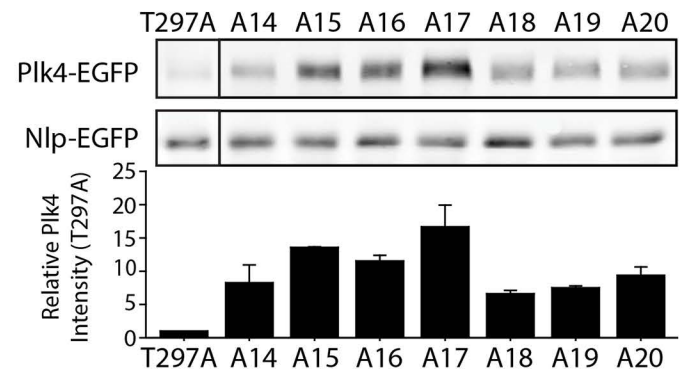
	271	276	285	287	290	293	297	300	301	303	306	311	315
WT:	LKC	S	S	S	S	S	D	F	S	S	Q	S	S
S293A:	LKC	S	S	S	S	S	D	F	S	S	Q	S	S
T297A:	LKC	S	S	S	S	S	D	F	S	S	Q	S	S
A14:	LKC	A	A	A	A	A	D	F	S	S	Q	S	S
A15:	LKC	A	A	A	A	A	D	F	S	S	Q	S	S
A16:	LKC	A	A	A	A	A	D	F	A	S	Q	S	S
A17:	LKC	A	A	A	A	A	D	F	A	S	Q	S	S
A18:	LKC	A	A	A	A	A	D	F	A	S	Q	S	S
A19:	LKC	A	A	A	A	A	D	F	A	S	Q	A	S
A20:	LKC	A	A	A	A	A	D	F	A	S	Q	A	A

Slimb-Recognition Motif (SRM)

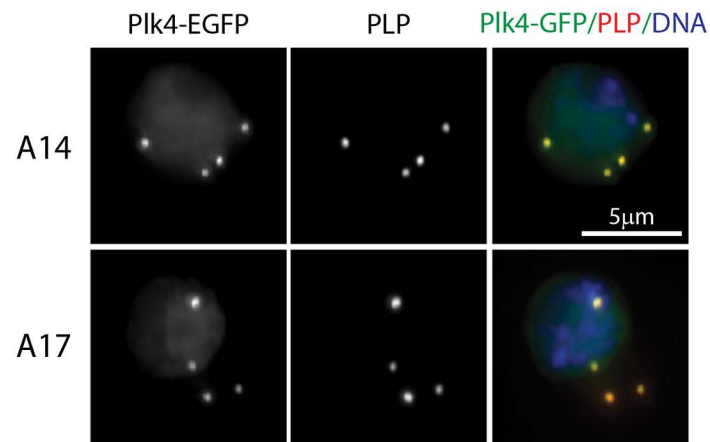
C



B



D



E

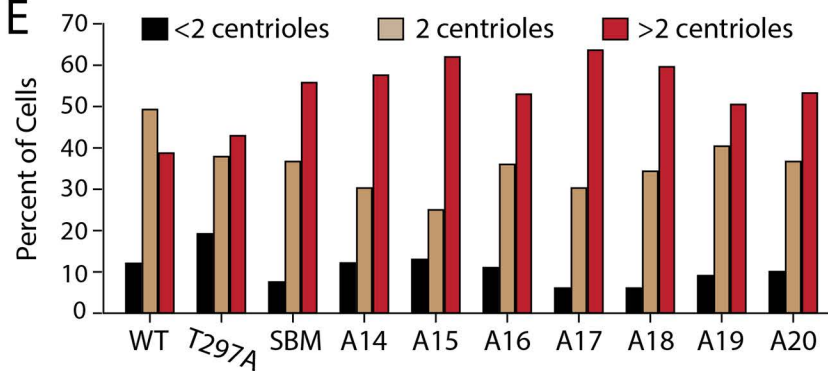


Figure S3. Hydroxyl Residues Flanking the S293 Contribute to Slimb Binding and Plk4 Stability

(A) A series of Plk4 constructs (A14-A20) was created by incrementally mutating all of the hydroxyl amino acids (blue) within the DRE, except S293, to alanines (red).

(B) Elimination of phosphorylatable residues within the DRE increases Plk4 levels even though the key residue, S293, is unaltered. (Top) Anti-GFP immunoblot of lysates prepared from S2 cells transiently co-expressing the indicated Plk4-EGFP mutant and Nlp-EGFP (loading control). (Bottom) The normalized Plk4 intensity values were obtained as described in the Figure 4B legend. Graphed values are relative to T297A. Data were acquired from three experiments.

(C) (Top) Anti-GFP immunoprecipitate of lysates from S2 cells transiently expressing 3xFLAG-Ubi and the indicated Plk4-EGFP mutant were probed with anti-GFP, FLAG, and Slimb antibodies. (Bottom) Plk4 ubiquitination levels and associated Slimb levels measured from the quantitative FLAG and Slimb immunoblots, respectively. Graphed values are relative to the WT-Plk4 control.

(D) S2 cells co-expressing the indicated Plk4-EGFP construct (green puncta) and Nlp-EGFP (green nuclei) were immunostained for PLP-centrioles (red). DNA (blue).

(E) Cells expressing different Plk4-EGFP constructs were immunostained as in (D) and their centrioles were counted. Graph shows the percentage of cells with the indicated number of centrioles per cell. Note that loss of hydroxyl DRE residues (not including S293) can have as large an impact on centriole amplification as expression of SBM-Plk4. Centrioles in 100 cells were measured per construct.

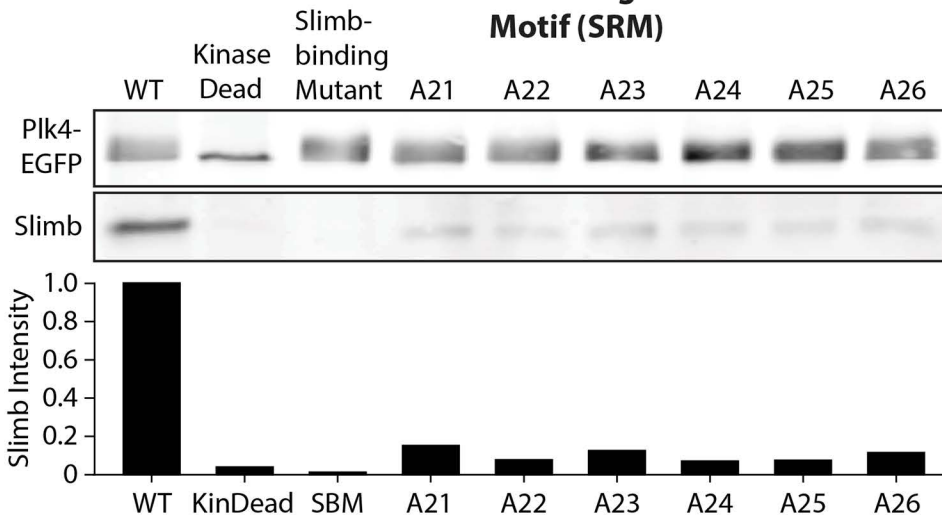
Figure S4

A

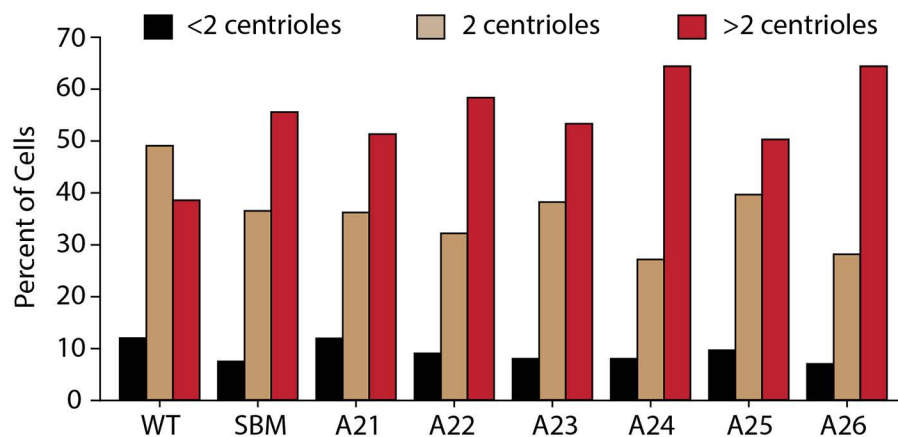
WT: LKC²⁷¹SNGGH²⁷⁶SAPGALNVF²⁸⁵SQSMESG²⁸⁷DSGIIT²⁹⁰FASSDSRNS²⁹³QQIRSVENS²⁹⁷SGP³⁰⁰303 306 311 315
 SBM: LKC²⁷¹SNGGH²⁷⁶SAPGALNVF²⁸⁵SQSMESG²⁸⁷DAGIIA²⁹⁰FASSDSRNS²⁹³QQIRSVENS²⁹⁷SGP³⁰⁰303 306 311 315
 A21: LKC²⁷¹ANGGH²⁷⁶AAPGALNVF²⁸⁵AQAMEAG²⁸⁷DSGIIT²⁹⁰FAASDSRNS²⁹³QQIRSVENS²⁹⁷SGP³⁰⁰303 306 311 315
 A22: LKC²⁷¹ANGGH²⁷⁶AAPGALNVF²⁸⁵AQAMEAG²⁸⁷DSGIIT²⁹⁰FAAASDRNS²⁹³QQIRSVENS²⁹⁷SGP³⁰⁰303 306 311 315
 A23: LKC²⁷¹ANGGH²⁷⁶AAPGALNVF²⁸⁵AQAMEAG²⁸⁷DSGIIT²⁹⁰FAAADARN²⁹³QQIRSVENS²⁹⁷SGP³⁰⁰303 306 311 315
 A24: LKC²⁷¹ANGGH²⁷⁶AAPGALNVF²⁸⁵AQAMEAG²⁸⁷DSGIIT²⁹⁰FAAADARNA²⁹³QQIRSVENS²⁹⁷SGP³⁰⁰303 306 311 315
 A25: LKC²⁷¹ANGGH²⁷⁶AAPGALNVF²⁸⁵AQAMEAG²⁸⁷DSGIIT²⁹⁰FAAADARNA²⁹³QQIRAVENS²⁹⁷SGP³⁰⁰303 306 311 315
 A26: LKC²⁷¹ANGGH²⁷⁶AAPGALNVF²⁸⁵AQAMEAG²⁸⁷DSGIIT²⁹⁰FAAADARNA²⁹³QQIRAVENAGP²⁹⁷300 303 306 311 315

Slimb-Recogniton Motif (SRM)

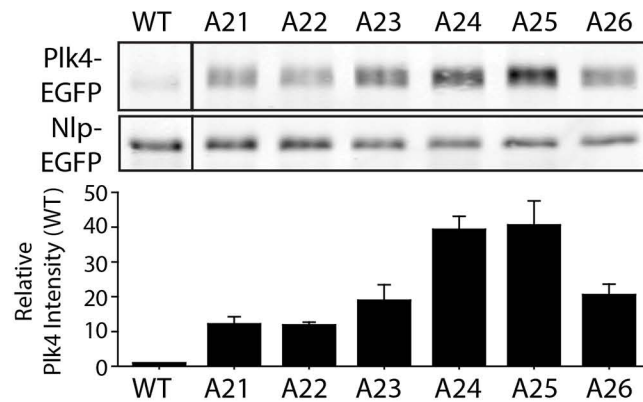
C



E



B



D

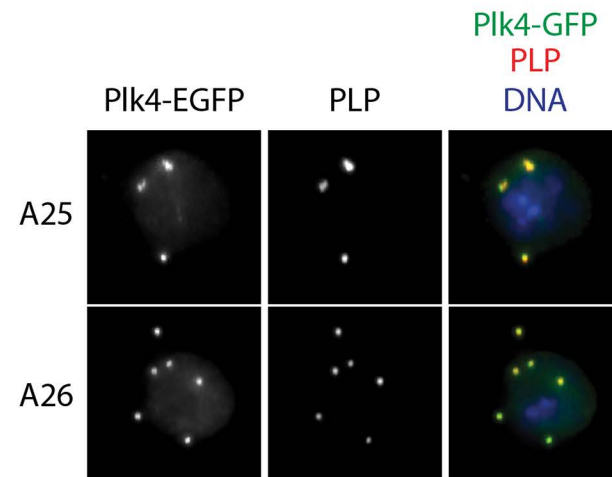


Figure S4. Hydroxyl Residues Flanking the SRM Collectively Contribute to Slimb Binding and Plk4 Stability

(A) A series of Plk4 constructs (A21-A26) was created by mutating all of the hydroxyl amino acids (blue) within the DRE, except for S293 and T297, to alanines (red).

(B) Elimination of phosphorylatable residues within the DRE increases Plk4 stability even when the SRM is unaltered. (Top) Anti-GFP immunoblot of lysates prepared from S2 cells transiently co-expressing the indicated Plk4-EGFP construct and Nlp-EGFP (loading control). (Bottom) Graphed values of normalized Plk4 intensities are relative to the WT-Plk4 treatment from three separate experiments.

(C) Elimination of about half the hydroxyl residues within the DRE diminishes Slimb binding by over 5-fold, even though the SRM is intact (compare A21 and WT). (Top) Anti-GFP immunoprecipitate of lysates from S2 cells transiently expressing the indicated Plk4-EGFP construct were probed with anti-GFP and Slimb antibodies. (Bottom) Slimb binding was measured by densitometry of the Slimb immunoblot and normalized to WT-Plk4.

(D) S2 cells co-expressing the indicated Plk4-EGFP plasmid (green puncta) and Nlp-EGFP (green nuclei) were immunostained for PLP (red) to mark centrioles. DNA (blue).

(E) S2 cells expressing the indicated Plk4 constructs were immunostained as in (D) and their centrioles counted. Graph shows the percentages of cells with the indicated numbers of centrioles per cell. Centrioles in 100 cells were measured per construct.

Table S1. *In vitro* phosphorylation sites of *Drosophila* Plk4 DRE. Partial list of recovered MS/MS peptides covering the DRE of *Drosophila* Plk4. Two autophosphorylated Plk4-kinase-DRE samples were analyzed by different facilities. The # symbol follows residues that are modified; all Ser/Thr modifications are phosphorylations. Note that not all recovered peptides are listed. Mascot parameters were obtained from Scaffold 4.0.7 (Proteome Software).

Modified S/T Residue	Peptide of DRE (amino acid residues 268-317)	Mascot ion score	Mascot identity score	Mascot delta ion score	Peptide Identification Probability	Sequest XCorr	Sequest deltaCN2
S271	(F)MLKCS#NGGHSAPGALNVF(S)	40.51	41.83	9.47	91		
S271	(L)KCS#NGGHSAPGALNVF(S)	41.45	42.02	7.99	91		
S276	(F)M#LKCSNGGHS#APGAL(N)	48.99	41.63	13.33	96		
S276	(F)MLKCSNGGHS#APGAL(N)	53.24	41.58	18.71	97		
S276	(F)M#LKCSNGGHS#APGALNVF(S)	60.61	42.01	19.68	98		
S276	(F)MLKCSNGGHS#APGALNVF(S)	51.17	41.85	16.52	97		
S276	(L)KCSNGGHS#APGALNVF(S)	54.25	42.02	32.77	98		
S285,T297	(F)S#QSM#ESGDSGIIT#F(A)	25.00	38.40	1.19	62		
S287	(F)SQS#M#ESGDSGIITF(A)	57.86	40.56	7.04	99		
S290	(F)SQSMES#GDSGIITF(A)	39.37	40.71	3.39	91		
S290	(F)SQSM#ES#GDSGIITF(A)	44.28	40.57	9.40	94		
S293	(F)SQSM#ESGDS#GIITF(A)	50.66	40.54	22.76	97		
S293,T297	(F)SQSMESGDS#GIIT#F(A)	33.12	38.78	14.20	85		
S290,S293	(K)CSNGGHSAPGALNVFSQSMES#GDS#GIITFASSDSR(N)					4.801	1
S293	(K)CSNGGHSAPGALNVFSQSMESGDS#GIITFASSDSR(N)					5.437	0.011
S293,T297	(K)CSNGGHSAPGALNVFSQSMESGDS#GIIT#FASSDSR(N)					5.463	1

S306	(R)NS#QQIR(S)					1.345	0.459
S311	(R)S#VENSGPDYK(D)					2.257	0.729
S311	(R)S#VENSGPDYKDDDDK(H)					2.807	0.733
S311	(R)S#VENSGPDYKDDDDKHHHHHH(-)					3.616	0.618
S311,S315	(R)S#VENS#GPDYK(D)					2.053	0.785
S311,S315	(R)S#VENS#GPDYKDDDDKHHHHHH(-)					3.156	0.581
S315	(R)SVENS#GPDYKDDDDKHHHHHH(-)					3.542	0.640

Table S2. *In vivo* phosphorylation sites of the *Drosophila* Plk4 DRE. Partial list of recovered MS/MS peptides covering the DRE of *Drosophila* Plk4. The # symbol follows residues that are modified; all Ser/Thr modifications are phosphorylations. Note that not all recovered peptides are listed. Parameters were obtained from Scaffold 4.0.7.

Modified S/T Residue	Peptide of DRE (amino acid residues 268-317)	Mascot ion score	Mascot identity score	Mascot delta ion score	Peptide Identification Probability
S271	(K)CS#NGGHSAPGALNVFSQ#SMESGDSGIITFASSDSR(N)	23.9	35.35	0.0	49
S285	(K)CSN#GGHSAPGALN#VFS#Q#SM#ESGDSGIITFASSDSR(N)	46.21	35.77	5.96	100
S285	(K)CSN#GGHSAPGALNVFS#QSM#ESGDSGIITFASSDSR(N)	59.77	36.04	1.32	100
S285	(K)CSN#GGHSAPGALN#VFS#Q#SM#ESGDSGIITFASSDSR(N)	65.74	35.50	0.73	100
S287	(K)CSN#GGHSAPGALNVFSQ#S#M#ESGDSGIITFASSDSR(N)	67.41	35.42	1.97	100
S287	(K)CSN#GGHSAPGALNVFSQ#S#M#ESGDSGIITFASSDSR(N)	78.26	35.54	0.10	100
S287	(K)CSN#GGHSAPGALN#VFSQ#S#M#ESGDSGIITFASSDSR(N)	31.53	35.67	1.38	87
S290	(K)CSN#GGHSAPGALNVFSQSM#ES#GDSGIITFASSDSR(N)	45.57	35.48	6.74	100
S290	(K)CSN#GGHSAPGALNVFSQ#SM#ES#GDSGIITFASSDSR(N)	65.15	35.95	4.56	100
S290	(K)CSN#GGHSAPGALNVFSQSM#ES#GDSGIITFASSDSR(N)	50.90	35.37	3.28	100
S290	(K)CSN#GGHSAPGALN#VFSQSM#ES#GDSGIITFASSDSR(N)	66.58	35.39	1.70	100
S290	(K)CSN#GGHSAPGALN#VFSQSM#ES#GDSGIITFASSDSR(N)	42.02	35.02	2.68	99
S293	(K)CSN#GGHSAPGALN#VFSQSM#ESGDS#GIITFASSDSR(N)	46.31	35.94	7.64	100
S293	(K)CSN#GGHSAPGALNVFSQSM#ESGDS#GIITFASSDSR(N)	55.56	35.05	6.73	100
S293	(K)CSN#GGHSAPGALNVFSQSM#ESGDS#GIITFASSDSR(N)	50.75	35.23	6.41	100
S306	(R)NS#QQIRSVENSGPQQVLPQIR(E)	38.48	31.75	2.59	99

S306	(R)NS#QQIRSVENSGPQQVLPQIREEFK(Q)	38.32	33.12	1.29	98
S311	(R)S#VENSGPQQVLPQIR(E)	45.47	30.60	19.47	100
S311	(R)S#VENSGPQQVLPQIR(E)	52.26	33.28	18.70	100
S311	(R)S#VENSGPQQVLPQIR(E)	49.99	30.58	17.13	100
S311	(R)S#VENSGPQQVLPQIR(E)	49.19	30.52	14.29	100
S315	(R)SVENS#GPQQVLPQIREEFK(Q)	76.25	32.49	28.13	100
S315	(R)SVENS#GPQQVLPQIR(E)	57.72	30.57	24.31	100
S315	(R)SVENS#GPQQVLPQIREEFK(Q)	35.47	34.94	21.72	95
S315	(R)SVENS#GPQQVLPQIR(E)	46.17	30.44	15.67	100

Supplemental Experimental Procedures

Cell culture and double-stranded RNAi (dsRNA Interference)

Drosophila S2 cell culture, in vitro dsRNA synthesis, and RNAi treatments were performed as previously described [27]. In brief, cells were cultured in Sf900II SFM media (Life Technologies). RNAi was performed in 6-well plates containing cells at 50–90% confluency by applying 10µg dsRNA in 1ml media and replenishing with fresh media/dsRNA every day for 4–5d. Control dsRNA was synthesized from control DNA template amplified from a non-GFP sequence of the pEGFP-N1 vector (Clontech) using the primers 5'-CGCTTTTCTGGATTCATCGAC-3' and 5'-TGAGTAACCTGAGGCTATGG-3' (all primers used for dsRNA synthesis in this study begin with the T7 promoter sequence 5'-TAATACGACTCACTATAGGG-3'). DNA template for Slimb dsRNA was generated using the primers 5'-GGCCGCCACATGCTGCG and 5'-CGGTCTTGTTCATTGGG to amplify a region of coding sequence from a Slimb cDNA.

Immunofluorescence microscopy

For immunostaining, S2 cells were fixed and processed exactly as previously described [27] by spreading S2 cells on concanavalin A-coated, glass-bottom dishes and fixing with 10% formaldehyde. Primary antibodies were diluted to concentrations ranging from 1 to 20µg/ml. They included rabbit and guinea pig anti-PLP [2]. Secondary antibodies (conjugated with Cy2, Rhodamine red-X, or Cy5 [Jackson ImmunoResearch Laboratories, Inc.]) were used at manufacturer-recommended dilutions. Hoechst 33342 (Life Technologies) was used at a final dilution of 3.2µM. Cells were mounted in 0.1M *n*-propyl galate, 90% (by volume) glycerol, and 10% PBS solution. Specimens were imaged using a DeltaVision Core system (Applied

Precision) equipped with an Olympus IX71 microscope, a 100× objective (NA 1.4), and a cooled charge-coupled device camera (CoolSNAP HQ2; Photometrics). Images were acquired with softWoRx v1.2 software (Applied Science).

Immunoblotting

S2 cell extracts were produced by lysing cells in cold PBS and 0.1% Triton X-100. Laemmli sample buffer was then added and boiled for 5 min. Samples of equal total protein were resolved by SDS-PAGE, blotted, probed with primary and secondary antibodies, and scanned on an Odyssey imager (Li-Cor Biosciences). Care was taken to avoid saturating the scans of blots. The integrated densities of fluorescent bands (measured from the digitized scans using ImageJ software [National Institutes of Health]) were normalized relative to the integrated densities of the corresponding loading controls. Transfected Nlp-EGFP (a constitutively-expressed nuclear protein; [3]) was used as loading control and transfection marker. Antibodies used for Western blotting include anti-Slimb [2], anti-GFP monoclonal JL8 (Clontech), anti-Myc (Cell Signaling Technologies) and anti-FLAG (Sigma-Aldrich) used at 1:1,000 dilutions. IRDye 800CW secondary antibodies (Li-Cor Biosciences) were prepared according to the manufacturer's instructions and used at 1:1,500 dilutions.

Constructs and transfection

Full-length cDNA of *Drosophila* Plk4 [3] was subcloned into a pMT vector containing in-frame coding sequence for EGFP (or Myc) and the inducible metallothionein promoter. QuikChange II (Agilent Technologies) was used according to manufacturer's instructions to generate the series of Plk4 mutants. Transient transfections of S2 cells were performed using a Nucleofector II and

nucleofector kit V (Lonza) according to manufacturer's instructions. Expression of all Plk4 constructs (and GFP control) was induced by addition of 50 μ M–2 mM copper sulfate to the culture medium. In Figure 1, addition of 50 μ M copper sulfate to cell medium was used to induce transgene expression to a low level, while 1mM copper sulfate was used to induce a high level of transgene expression.

Immunoprecipitation

Polyclonal and monoclonal antisera were bound to equilibrated protein A (or protein G) Sepharose (Sigma-Aldrich) by gently rocking overnight at 4°C in 0.2 M sodium borate. In some cases, the prebound antibody was cross-linked to the resin by incubating with 20mM dimethyl pimelimidate dihydrochloride in PBS, pH 8.3, 2 h at 22°C, and then quenching the coupling reaction by incubating with 0.2 M ethanolamine, pH 8.3, 1 h at 22°C. Antibody-coated beads were washed three times with 1.5 ml of cell lysis buffer (CLB; 50 mM Tris, pH 7.2, 125 mM NaCl, 2 mM DTT, 0.1% Triton X-100, and 0.1 mM PMSF). Transfected cells expressing recombinant proteins were lysed in CLB, and the lysates clarified by centrifugation. Antibody-coated beads were rocked with lysate for 1 h at 4°C, washed two times with 1 ml CLB, and then boiled in Laemmli sample buffer. For GFP immunoprecipitations, GFP-binding protein (GBP) [28] was fused to the Fc domain of human IgG (pIg-Tail) (R&D Systems), tagged with His₆ in pET28a (EMD Biosciences), expressed in *E. coli* and purified on HisPur resin (ThermoFisher) according to manufacturer's instructions. Purified GBP was bound to Protein A-coupled Sepharose, and then cross-linked to the resin using the method described above. In vivo ubiquitination assays were performed by co-expressing Plk4-EGFP constructs with triple FLAG-tagged *Drosophila* ubiquitin (CG32744) (also under the metallothionein promoter and Cu-

induced) and then probing the immunoblot of the cell lysate with anti-FLAG antibody (Sigma-Aldrich).

In Vitro Autophosphorylation of Plk4

Drosophila (His)₆-tagged Plk4 kinase domain + DRE (amino acids 1-317) was cloned into the pET28a vector, expressed in BL21DE3 bacteria, and purified on HisPur resin (ThermoFisher) according to manufacturer's instructions. Purified Plk4 was autophosphorylated by incubating with 50μM ATP, 1-2 h, 25°C, in reaction buffer (40mM Na HEPES, pH 7.3, 150mM NaCl, 5mM MgCl₂, 0.5mM MnCl₂, 1mM DTT, 0.1mM PMSF, 10% glycerol). (To identify phosphorylated residues that are not generated by autophosphorylation, a sample of the same purified Plk4 is left untreated.) Samples were resolved by SDS-PAGE, Coomassie stained, and then processed for mass spectrometry (below).

Mass Spectrometry

Mass spectrometry was performed at the Taplin Mass Spectrometry Facility (Harvard Medical School) and the NHLBI Proteomics Core Facility (NIH). Better coverage of Plk4 was obtained by the NHLBI facility using the following procedure. Samples were reduced (10μM dithiothreitol, 55°C, 1hr), alkylated (55mM iodoacetamide, room temperature, 45min), and trypsin digested (~1μg trypsin, 37°C, 12hrs) in-gel, and then extracted. Peptide samples were loaded onto a Zorbax C₁₈ trap column (Agilent Tech., Santa Clara, CA) to desalt the peptide mixture using an on-line Eksigent (Dublin, CA) nano-LC ultra HPLC system. The peptides were then separated on a 10 cm Picofrit Biobasic C₁₈ analytical column (New Objective, Woburn, MA). Peptides were eluted over a 90 min linear gradient of 5-35% acetonitrile/water containing

0.1% formic acid at a flow rate of 250 nL/min, ionized by electrospray ionization (ESI) in positive mode, and analyzed on a LTQ Orbitrap Velos (Thermo Electron Corp., San Jose, CA) mass spectrometer. All LC MS analyses were carried out in “data-dependent” mode in which the top 6 most intense precursor ions detected in the MS1 precursor scan (m/z 300-2000) were selected for fragmentation via collision induced dissociation (CID). Precursor ions were measured in the orbitrap at a resolution of 60,000 (m/z 400) and all fragment ions were measured in the ion trap.

LC MS/MS data acquired from tryptic digests were searched independently using the MASCOT algorithm. All data were searched against the *Drosophila* NCBIInr protein database for peptide and protein identifications. Trypsin or chymotrypsin was specified as the digestion enzyme, allowing for up to 2 missed cleavage sites. Carbamidomethylation (C) was set as a static modification and Oxidation (M) and Phosphorylation (S,T,Y) were selected as variable modifications. Precursor and fragment ion mass tolerances were set to 20 ppm and ± 0.8 Da, respectively. Following MASCOT searches, database search results were combined to obtain a comprehensive map of all peptides identified from Plk4.

Statistical Analysis

The statistical significance of differences in average measurements was evaluated using one-way ANOVA and Dunnett’s multiple comparisons post-test (GraphPad Prism 6.0). Reported P values are adjusted for multiplicity. Differences in averages are deemed significant if $P < 0.05$.